SLAC-PUB-15638

Beam Ion Instability in SPEAR3: Measurements, Analyses and Simulations

L. Wang, J. Safranek, Y. Cai, J. Corbett, B. Hettel, T. O. Raubenheimer, J. Schmerge and J. Sebek, SLAC

Abstract

Weak vertical coupled bunch instability with oscillation amplitude at order of a few μm level has been observed in SPEAR3 at nominal vacuum pressure. The instability becomes stronger when there is a vacuum pressure rise by partially turning off vacuum pumps and it becomes weaker when the vertical beam emittance is increased by turning off the skew quadrupole magnets. These confirmed that the instability was driven by ions in the vacuum. This paper presents the comprehensive measurements, simulation and analysis of the beam ion instability in SPEAR3. The effects of vacuum pressure, beam current, beam filling pattern, chromaticity, beam emittance are investigated in great detail. Our analyses and simulations with multiple gas species and realistic beam optics agree well with the measurements.

PACS numbers: 29.27.Bd, 29.20.Dh

I. INTRODUCTION

In an electron accelerator, ions generated from the residual gas molecules can be trapped by the beam. Then these trapped ions interact resonantly with the beam and cause beam instability and emittance blow-up. Most existing light sources use a long single bunch train filling pattern, followed by a long gap to avoid multi-turn ion trapping. However, such a gap does not preclude ions from accumulating during one passage of the single bunch train beam, and those ions can still cause a Fast Ion Instability (FII) as predicted by Raubenheimer and Zimmermann [1]. FII has been observed in ALS[2] and PLS[3,4] by artificially increasing the vacuum pressure by injecting helium gas into the vacuum chamber [2,3,4] or by turning off the ion pumps [3] in order to observe the beam ion instability. However, when the beam emittance becomes smaller, the beam ion instability can occur at nominal vacuum pressure as observed in PLS [5], SOLEIL [6], and SSRF [7].

Although the beam ion instabilities have been qualitatively observed in many accelerators, there is still a shortage of quantitatively agreements with theory and simulation. This paper provides detail comparisons of the measurements with analyses and simulations. Our analysis can handle multiple gas species vacuum, realistic beam optics, nonlinear space charge force and chromaticity simultaneously. All these factors provide damping to the beam

Work supported in part by US Department of Energy under contract DE-AC02-76SF00515.

SLAC National Accelerator Laboratory, Menlo Park, CA 94025

ion instability. The existing beam ion instability theories usually include single damping factor only. For instance, Stupakov [8] studied the effect of the variation of beam size along the accelerator. Kim-Ohmi model [9] and Wang [10] includes the nonlinear space charge effect. All previous theories are for single gas species vacuum and zero chromaticity. Our integrated multi-physics analysis method ensures fairly good agreements of our analyses with the measurements.

The beam ion instability typically has very small oscillation amplitude. If other beam instabilities exist, the beam ion instability will be not easy to be distinguished. In SPEAR3, there is no coupled bunch instability driven by resistive wall impedance and High Order Modes (HOMs) and the beam emittance is low. This makes SPEAR3 an ideal machine for the measurement of the beam ion instability. This paper reports the measurements of beam ion instabilities in SPEAR3 during a period of one year, which includes single bunch train instability (FII) and multi-bunch train instability. Note that the instability may be not the same even with the same beam due to the change of the vacuum with time. All the measurements are done with good vacuum pressure except one case with rising vacuum pressure artificially by turning off the vacuum pump.

The natural emittance of SPEAR3 beam is 10 *nm* and there is a low vertical emittance of 1*4 pm*. The vertical emittace is lower as 10 *pm* during the recent operation. It can be corrected as low as 5 *pm*. SPEAR3 has a circumference of 234 *m* with a harmonic number of 372. The nominal beam filling pattern is six bunch-trains with total 280 bunches and there is no beam ion instability with the nominal beam. Table 1 lists the main parameters of SPEAR3. The vacuum of SPEAR3 ranges from 0.1 to 0.5 *nTorr*, which varies from section to section.

It is important to know the important characters of the beam ion instability in order to explain the measurements. The ions are trapped by the electron beam and oscillate with a frequency depending on beam current and the transverse size of electron beam, which varies along the ring. The ion frequency ranges from 10MHz to 150MHz for SPEAR3 beam, which correspond to an oscillation period of 100 ~ 6 *ns*. Since this ion oscillation period is much longer than the bunch spacing of 2 *ns*, the slowly moving ions disturbed by previous electron bunch can couple the perturbation to the following electron bunches and therefore causes coupled bunch instability with unstable mode number correlated with the ion oscillation frequency. The dependence of unstable mode number on the beam current and transverse beam size is one important characteristic of the instability driven by ions.

Different from other types of beam instabilities, the amplitude of the unstable bunches driven by ions normally saturates at roughly the beam size due to the strong nonlinear space charge effect at large amplitude. The beam ion

instability grows quickly in the linear regime. However, the amplitude of the unstable beam at saturation is always small, for instance about 10 μm in SPEAR3. This is another important characteristic of the beam ion instability.

This paper is organized as follows. The measurements, analysis and simulation are presented in sections II, III, and V, respectively. One may read the analysis part first for deeper understanding of the measurements. The beam ion instability can be well explained by the impedance of the ion cloud.

Table 1 Typical Parameters of SPEAR3

Physics	Symbol/Unit	Value
Horizontal Emittance	ε_x (nm)	10
Vertical Emittance	ε_y (pm)	14
Beam Current	I (mA)	200-500
Bunch Number	M	280
Bunch Length	σ_z (mm)	6
Harmonic Number	h	372
Beam Energy	E (GeV)	3
Circumference	C (m)	234
Bunch spacing	S_b/c (ns)	2.1
RF frequency	f_{RF} (MHz)	476.315
Revolution frequency	f_0 (MHz)	1.280
Horizontal tune	ν_x	14.1
Vertical tune	ν_y	6.18
Momentum compaction factor	α	1.6×10^{-3}
Energy Spread	σ_E	9.8×10^{-4}
Radiation Damping time	$\tau_x/\tau_y/\tau_z$ (ms)	4.0/5.3/3.2
Vacuum pressure	P ($nTorr$)	0.1~0.5

II. MEASUREMENTS

2.1 Dependence on vacuum pressure

The beam-ion instability was first observed in 200 mA operation with a single bunch train filling pattern. Fig. 1 shows the observed typical beam spectrum. The high peak signals are the revolution frequencies and the low peaks are the vertical low sidebands. The unstable modes of these low vertical sidebands agree with the theoretical prediction. There are no horizontal sidebands in all the cases. Fig. 2 shows the vertical beam oscillation amplitude along the bunch train. The beam has single bunch train with 280 bunches. A bunch with large bunch current is filled in the middle of train gap as a probe. Therefore, it is not pure single bunch train beam. The observed bunch oscillation amplitude increases, but not exactly monotonically, along the bunch train and saturates at just one times

of beam size. The coupled bunch instability driven by traditional impedance doesn't have such saturation mechanism. This indicates the observed instability is driven by the ions in the vacuum.

In order to directly confirm that the vertical instability is driven by ions, the vacuum pressure was raised by partially turning off vacuum pumps. Fig. 3 shows the vertical low sidebands at different average vacuum pressures along the ring with 300 *mA* total beam current. The measurements in this paper have been done above the RF frequency and the frequencies of sidebands in all plots are the difference of the sideband frequency with the RF frequency. The beam fill pattern was a six bunch train, and there was no vertical beam instability at ring average pressure 0.37 *nTorr* when all vacuum pumps were on. The instability appeared as the pressure increased, and it became stronger with a higher pressure. This directly confirms that the observed vertical instability is driven by ions in the vacuum chamber.

The oscillation frequency of trapped ions varies along the accelerator ring due to the variation of the beam size. A larger variation of the beam size along the ring causes a broader distribution of the unstable modes. The ion frequency also varies with the mass of the ions. The existing of multiple gas species in the vacuum increases the total variation of the ion frequency and therefore makes the distribution of the ion frequency even broader. In general, a broad beam spectrum of unstable modes is expected for beam ion instability. This is clearly seen in Fig. 3 and other results shown later. Once again, the amplitude of the sidebands is always small, even with high vacuum pressure.

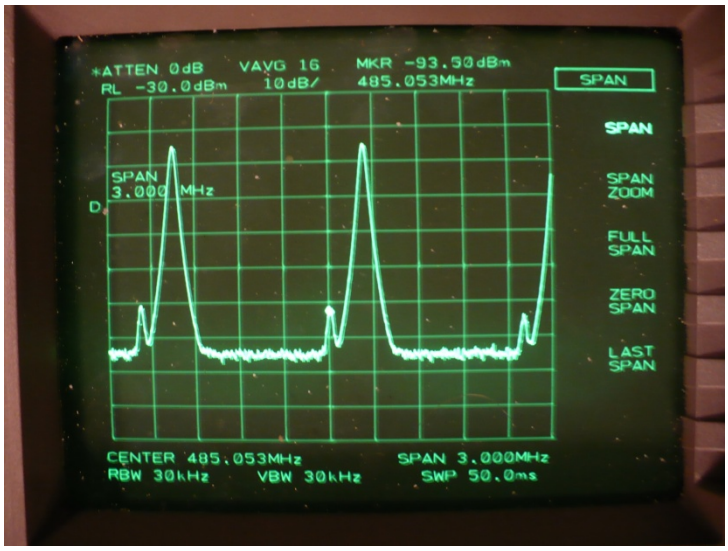

FIG. 1. Beam spectrum at 200 *mA* with a single bunch train filling pattern. The high peaks are the revolution harmonics and the low peaks are the vertical lower sidebands.

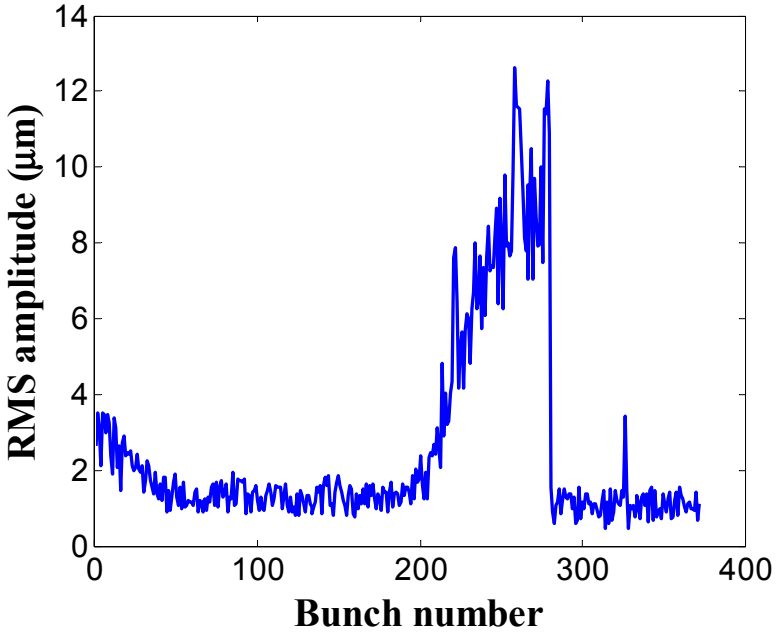

FIG. 2. Snapshot of measured beam's vertical oscillation amplitude with single bunch train filling pattern at one particular moment. Bunches 1-280 and 326 are filled with a total beam current of 200 *mA*.

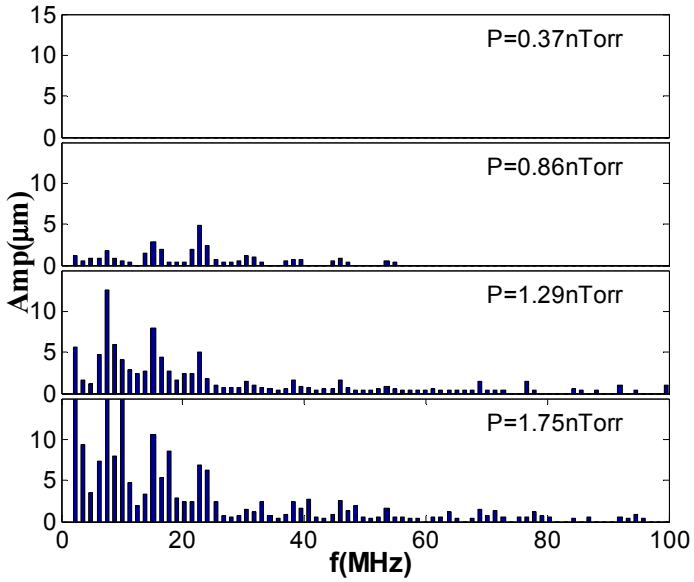

FIG. 3. Observed vertical lower sidebands at different vacuum pressures. The beam consists of six bunch trains with total bunch number of 280. The beam current is 300 mA. There are no sidebands with the nominal pressure of 0.37 *nTorr*. The vacuum pressure is increased by partially turning off the ion pumps.

2.2 Dependence on beam emittance

Further tests have been carried out to confirm the vertical emittance effect expected for ion instabilities. All skew quadrupole magnets were turned off to increase the vertical emittance. Fig. 4 shows the measured vertical lower sidebands observed on the beam spectrum analyzer when the skew quadrupole magnets were on and off. The beam consists of a single bunch train with a total beam current of 192 *mA*. When the skew quadrupole magnets were off, the maximum frequency of the observed sidebands reduced from 26.0 *MHz* to 13.0 *MHz*, and the maximum amplitude also dropped as predicted by the theory. This also indirectly confirms that the instability is driven by ions in the vacuum, instead of the impedance inside the vacuum chamber, because the resistive wall and geometric impedance doesn't change with the beam emittance. The observed frequencies also agree with the estimation shown later. Hydrogen doesn't contribute to the instability although it is the dominant gas species in the vacuum chamber. We rarely observe beam instabilities at the higher frequencies expected from Hydrogen ions even with high beam current. Very weak signal appears at that frequency range sometimes. This can be explained by its small ionization cross-section. Furthermore the bunch train gap is more effective in reducing the ion density for light ions, which also reduces the effect of light ions. Generally speaking the heavy ions are more important for the beam ion instability due to their large ionization cross-section and stable motion. More preciously speaking, the heavier ions contribute to larger impedances as shown later.

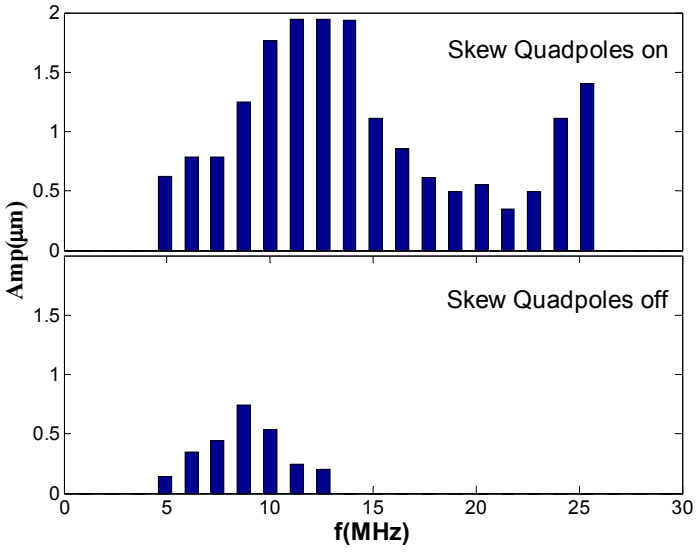

FIG. 4. Observed vertical lower sidebands in a single bunch train filling pattern with 280 bunches and total beam current of 192 mA for different beam coupling, when skew quadrupole magnets are on and off.

2.3 Beam current effects

Beam current affects the instability in two ways: the frequencies of the unstable modes increase with the square root of the beam current, and the instability growth rate increases linearly with beam current (with the assumption of a constant vacuum and long enough bunch train gap). Fig. 5 shows the vertical sidebands for various beam currents. The beam has single bunch train. There is a stronger instability at higher beam current. Other types of beam instability also have the same character. However, the amplitude of the unstable mode is always small (less than 5μm here), which is the typical feature of beam ion instability. The increment of the unstable modes' frequencies with beam current is also the character of the beam instability driven by ions. Note that the unstable modes with lower frequency always appear when a strong instability occurs, for instance with a higher beam current, higher vacuum pressure, a shorter bunch train gap. When the amplitude of the beam instability becomes larger than the beam size, the oscillation is in a nonlinear regime which results in a larger frequency spread.

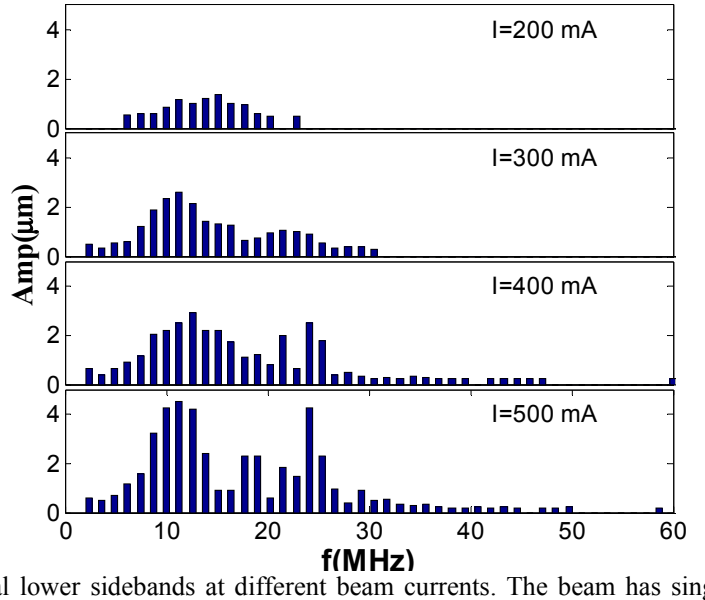

FIG. 5. Observed vertical lower sidebands at different beam currents. The beam has single bunch train with 280 bunches.

2.4 Beam filling pattern effect

The beam ion instability is sensitive to the beam filling pattern, because the accumulation of the ions depends on the beam filling pattern. For instance, more ions can survive from a shorter bunch train gap. Most light sources run with a single bunch filling pattern followed by a long gap to avoid multi-turn ion trapping. The instability in SPEAR3 becomes slightly stronger when the train gap is reduced from 189 *ns* to 38 *ns*. However, it is much stronger when the gap is reduced from 38 *ns* to 17 *ns*. This suggests that the effect of gap is strongly nonlinear, a gap of 38 *ns*

is tolerable but a gap of 17 *ns* is too short. This result qualitatively agrees with the simulation which shows an exponential decay of the ion density during the bunch train gap. A blowup of vertical beam size is also observed with short gap as shown in Fig. 6. The pictures are taken by the pin-hole camera from the beam line.

A multi-bunch train filling pattern can mitigate the instability by reducing the number of ions trapped by the beam [10]. Fig.7 shows the vertical oscillation amplitude of the unstable modes with one, four and six bunch trains. The beam current is 500 *mA* in all the cases. There is significant reduction with four bunch trains compared with a single bunch train. However, the reduction speed becomes small beyond four bunch trains. The optimized beam filling pattern is six bunch trains, which is chosen as the SPEAR3 nominal operation mode. The bunch train gap at six bunch train filling pattern is 32 *ns*, which is equal to one wavelength of the frequency of 31 *MHz*. The frequency of most unstable modes is below 31*MHz* as shown in Fig. 7. This measurement suggests that the optimized train gap is just about 1~2 ion oscillation wavelength. The beam is unstable with single bunch train beam filling at 200 *mA* beam current as shown in Fig. 1. However, the instability disappears when the single bunch train is divided into two equal bunch-trains.

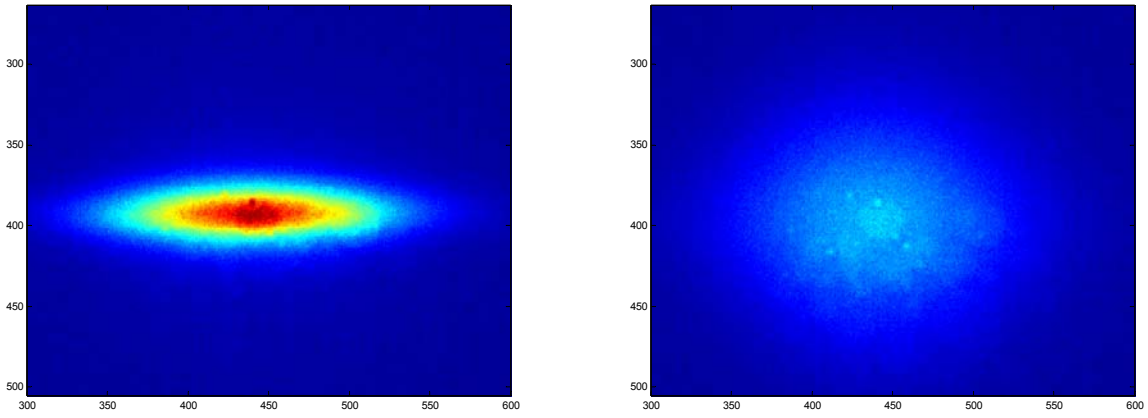

FIG. 6. Beam profile with different bunch train gap: 42 ns spacing (left) and no gap (right). The beam has a one bunch-train filling pattern with beam current of 200mA.

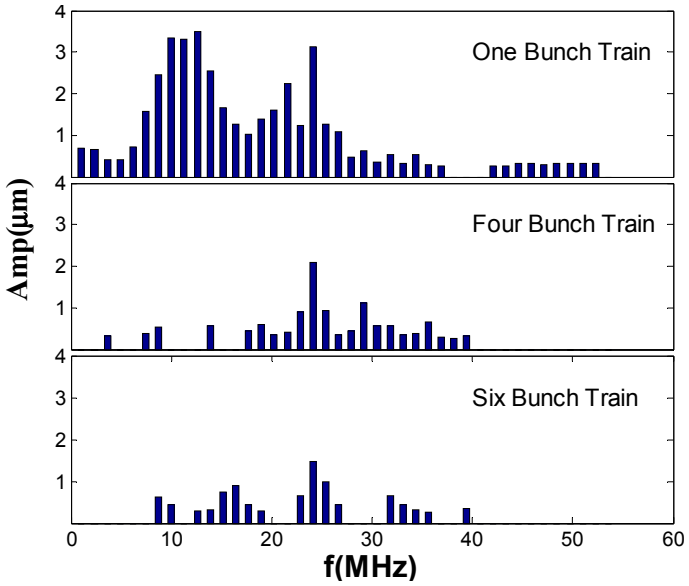

FIG.7. Oscillation amplitude of beam's vertical lower sidebands for different beam filling patterns: one, four and six bunch trains. The total beam current is 500 *mA* with a total bunch number of 280 in all cases. The horizontal and vertical chromaticity is 1.6 and 2.0, respectively.

2.5 Chromaticity effect

Besides multi-bunch train filling patterns, the instability can also be mitigated by a larger chromaticity. Fig. 8 shows the observed vertical low sidebands driven by ions at different vertical chromaticity in SPEAR3. The beam has a single bunch train, which consists of 280 bunches with a total beam current of 500*mA*. The horizontal chromaticity is 2.0 in all cases. It clearly shows the damping effect due to a large chromaticity. However, the beam life time drops from 10 hours to 4.7 hours when the chromaticity increases from 2.0 to 7.0. A larger chromaticity can also reduce the beam injection rate. SPEAR3 is operated with continuous beam injection to keep the beam current constant. The beam is injected every five minutes. Therefore, the mitigation of beam ion instability with a large chromaticity may be limited in practice due to its side effects.

SPEAR3 normally runs with four or six bunch trains. The instability at 500mA beam current with six bunch trains is completely suppressed by increasing the vertical chromaticity from 2.0 to 2.6. Therefore, the beam ion instability in SPEAR3 is not a problem even without feedback. A feedback may become necessary for future low emittance upgrade. When beam ion instability appears, which often happens at the beginning of a run after a long shut down, a slightly higher vertical chromaticity is used to completely suppress the instability. For instance, we

once observed vertical sideband and also a beam size blow-up from pinhole camera at the beam line 2 with 350 *mA* total beam current, a increment of the vertical chromaticity does suppress the dipole instability and emittance below-up.

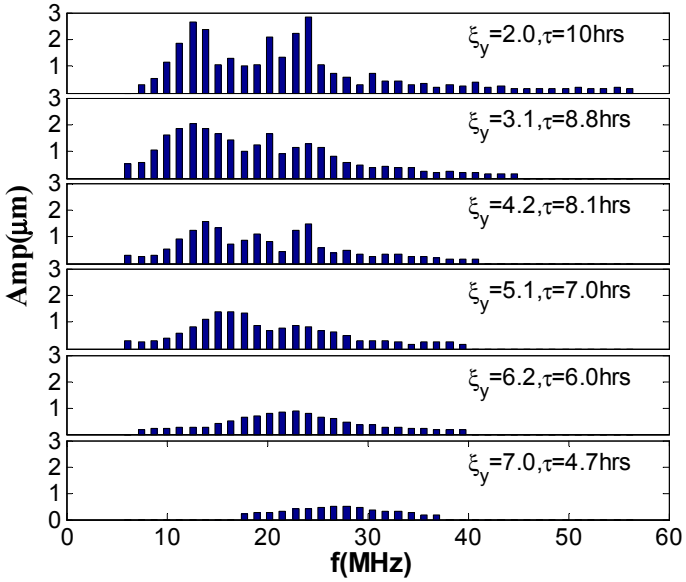

FIG. 8. Observed oscillation amplitude of beam's vertical lower sidebands with varying vertical chromaticity in SPEAR3. The beam has a single bunch train, which consists of 280 bunches with a total beam current of 500 *mA* in all the cases. The lifetime is also shown in the plot.

III. ANALYSIS

3.1. Impedance of an ion cloud with arbitrary vacuum and beam optics

To compare with the measurements, it is essential to accurately model the realistic multiple gas species vacuum and the variation of the beam size along the ring. The existing beam ion instability theories don't have such capability. Our analysis can handle multiple gas species vacuum, realistic beam optics, nonlinear space charge force and chromaticity simultaneously. Therefore, it can be directly used to compare with our measurements.

The beam ion instability is two-stream beam instability. The ions generated by gas ionization are trapped by a negative charged beam (electron beam here). In the linear regime, the coupling force between the two-stream electron-ion beams can be described by a wake function. When the wavelength of the ion oscillation is much longer then the bunch spacing, the wake field of an ion-cloud with a constant beam size is given by [10]

$$W_y(s) = \hat{W}_y \, e^{-\frac{\omega_i s}{2Q_0 c}} \sin(\frac{\omega_i s}{c}), \tag{1}$$

with the amplitude of the wake as

$$\hat{W}_y = N_i\left(\frac{r_p S_b}{AN_e}\right)^{1/2}\left[\frac{4}{3}\frac{1}{\sigma_y(\sigma_y+\sigma_x)}\right]^{3/2}. \tag{2}$$

Where ω_i is the ion frequency, c is the speed of light, r_p is the classical radius of proton, A is the mass number of the ion, N_i is the number of ions, N_e is electron bunch population, S_b is bunch spacing and $\sigma_{x,y}$ is the transverse root mean square (*rms*) beam size of the electron bunches. Q_0 is the quality factor due to the nonlinear space charge field, which depends on the distribution of the particles. It is about 9 by simulation for a Gaussian distributed beam [10]. The nonlinearity has weak dependence on the vertical beam emittance when the horizontal emittance is fixed. For instance, the Q_0 value changes from 8.63 to 9.74 when the vertical emittance is increased from 1 *nm* to 8 *nm* in our simulation. The nonlinearity of the fields with other distributions can also be estimated numerically.

The wake field of an ion beam represents the space charge force between the ion-electron beams. But it is different from the traditional space charge wake and impedance. For the two-stream electron-ion beams, the leading electron bunch affects the following one via the ion beam. As a result, the wake function of the two-stream beams depends on the charge and distribution of the two beams. Note that the distribution of ion cloud is not exactly Gaussian distribution, but the electric field of the ion-cloud closely approximates that of a Gaussian distribution. The wake function given in Eqs.(1-2) is based on this approximation and it slightly underestimates the wake function of ion cloud [10]. For a flat beam as in most electron rings, the vertical wake function is larger than the horizontal one. Therefore, there is a stronger instability in the vertical plane. This explains the reason we observed the vertical instability only. In the rest of this paper we will discuss about the instability in the vertical direction only and omit the subscript *y* in some variables for simplicity. The coherent ion oscillation frequency is

$$\omega_{i,y} = 2\pi f_{i,y} \approx c\left(\frac{4N_e r_p}{3AS_b(\sigma_x+\sigma_y)\sigma_y}\right)^{1/2}, \tag{3}$$

In general the beam size varies along the ring and the vacuum pressure can also be different from section to section along the ring. The total wake field from the ions can be accurately calculated from the integral around the whole ring as [10]

$$W_{ring}(s) = \int_0^C \frac{4}{3}\frac{\omega_{i,y}(z)}{c}\frac{\lambda_i(z)S_b}{N_e}\frac{1}{\sigma_y(z)(\sigma_y(z)+\sigma_x(z))}e^{-\frac{\omega_i(z)s}{2Q_0c}}\sin\left(\frac{\omega_i(z)s}{c}\right)dz. \tag{4}$$

Where λ_i is the ion line density. The volume density of ion-cloud increases linearly along the bunch train and

exponentially decays during the bunch train gap with a decay time of the order of ion oscillation period [10]. Therefore, the above equation can be used to calculate the wake function with arbitrary beam filling pattern. In Eq.(4), it is assumed that the bunch spacing is much shorter than the ion oscillation period along the whole ring. This condition should be checked at each location and the integral should be done only at the locations where this assumption is true. For instance, there is very small betatron function in the wiggler section of the ILC damping ring, the light ions species can't be trapped along the bunch train. The strong space charge force of the electron bunch can over kick the ions and instantly drives the ions out of the bunch central area.

The total wake function with multiple gas species can be calculated from Eq. (4) by linearly adding the wake function of different ion species together. As a result, Eq. (4) gives the total wake function of ions along the ring with arbitrary beam optics and vacuum, which also includes the nonlinear space charge effect. It should be pointed out that it is essential to calculate the wake function using the integral in Eq. (4). The wake function can be very inaccurate if it is estimated by assuming a constant beam size along the ring as is shown later.

The vacuum of different accelerators varies. In SPEAR3 vacuum, the dominant gas species are H_2 (48%), H_2O (21%), CO_2 (14%), CO (12%) and CH_4 (5%). They are the average values of four vacuum gauge data. We will use this vacuum component through this paper.

In most cases, it is clearer to look at the problem in frequency domain. The beam ion instability growth rate is proportional to the impedance as shown later. The total impedance due to the ion cloud along the whole ring can be obtained by Fourier Transform of the wake function as

$$Z_{\perp}(\omega) = i\int_{-\infty}^{\infty} \frac{ds}{c} W_{ring}(s) e^{i\omega s/c} \quad . \tag{5}$$

The wake function and the impedance including all effects (nonlinear space charge force, beam optics and multiple gas species) in SPEAR3 for a total pressure of 0.37 *nTorr* is shown in Fig.9. The beam filling pattern consists of six bunch trains and a total beam current of 500 *mA*. The ion density seen by different bunches varies when the beam is not uniformly distributed. The wake function is calculated using the average ion density seen by all bunches. To improve comprehension of the physics, the wake function and the impedance induced by different ion species are presented in order to compare the instability driven by different ion species. A quality factor Q_0 of 9 is used. The wake function of the CO_2 ion species has the largest amplitude due to its large ionization cross-section and small diffusion rate during the train gap because of its large mass. H_2 ion species has the second largest wake function due to the largest contribution to the vacuum pressure. The wake functions of each type ions in Fig. 9a still

have resonance form. The wavelength of wake functions is longer than the bunch spacing. Therefore they can cause couple bunch instability.

The shape of impedance spectrum for single gas species, as shown in Fig 9b, depends on the variation of the beam size along the ring. The impedances at different frequency are the contributions of the ions from different locations of the ring where the electron bunches have different beam size. Therefore, the impedance spectrum (the frequency information) represents the variation of the beam size along the whole ring and it characterizes the beam optics effect. Note that the relative frequency spread $\Delta\omega/\omega$ of the impedance induced by different ion species is the same. An accelerator ring with a large variation in beam size, such as ILC damping ring [11], causes a large frequency spread in the ion impedance and therefore a large damping to the beam ion instability.

Similar to the beam optics effect, the multi-gas species can also contribute to an additional spread in the ion frequency, as shown in Fig. 9b. The overlapping of the frequencies of different types of ions species increases the overall ion frequency spread and therefore it further mitigates the instability. Note that the frequency of H_2 ions is well separated from the frequencies of other ion species. The frequencies of CH_4, H_2O, CO and CO_2 ion overlap each other with a range from 20 *MHz* to 60 *MHz*. Therefore it is not possible to distinguish the ion species from the frequency in that range as shown in the experiment. The overlapping of the frequencies of different ions provides a broad spectrum.

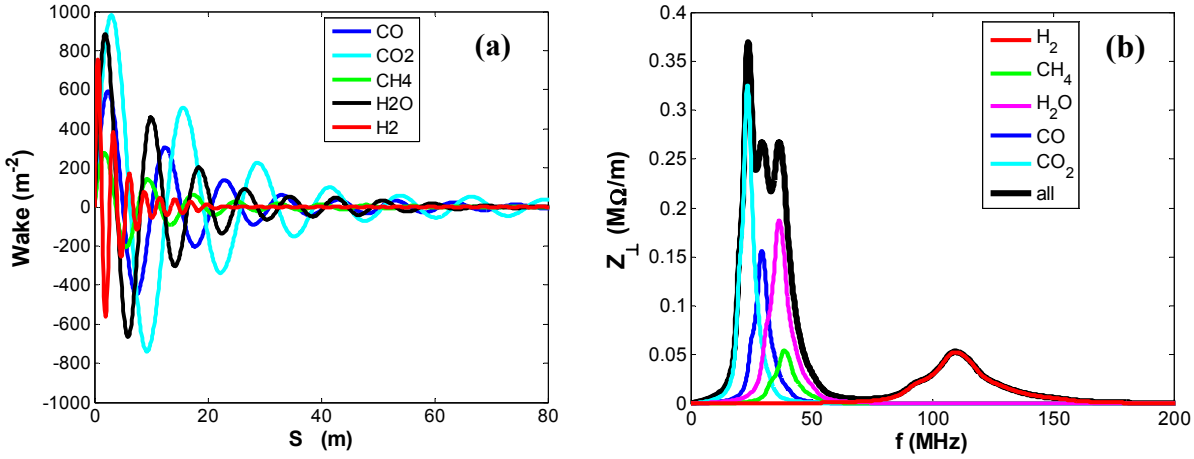

FIG.9. Vertical wake function (a) and real part of impedance (b) due to different ion species in SPEAR3 with total pressure of 0.37 *nTorr*. The beam filling pattern consists of six bunch train and a total beam current of 500 *mA*. The total bunch number is 280.

3.2. Instability driven by multiple gas species

When the beam is evenly filled along the ring, the exponential growth rate of the coupled bunch instability for mode $y_j^{\mu} \propto e^{2\pi\mu j/n_b}$ is given by the imaginary of the coherent frequency shift with mode number μ [12]

$$\Omega_{\mu} - \omega_{\beta} = i\frac{N_e M r_e c}{2\gamma T_0^2 \omega_{\beta}} \sum_{p=-\infty}^{\infty} Z_{\perp}((pM + \nu_y + \mu)\omega_0) \ . \tag{6}$$

Here T_0 and ω_0 are the revolution period and frequency, ν_y is the betatron tune, M is the bunch number and r_e is the classical radius of electron and ω_β is the betatron frequency. The real part of the frequency shift gives the tune shift due to ion cloud and the imaginary part gives the exponential growth rate of the coupled bunch instability. The growth time of the instability is the inverse of the growth rate. A multi-bunch train beam filling pattern with short train gaps is an effective way to mitigate the beam ion instability. We will use the formulae above to estimate the beam ion instability of multi-bunch train beam with the approximation of a uniformly distributed beam.

Fig. 10 shows the growth rate of the unstable modes driven by ions with the impedance shown in Fig. 9(b). The contributions of different types of ions are clearly shown in the plot. CO_2, CO and H_2 contribute to the most unstable modes. The actual instability is very weak in this case if considering the radiation damping effect as shown by the dashed line in the plot. The unstable modes driven by Hydrogen ion are completely damped by the radiation damping although Hydrogen gas is the dominant species in the SPEAR3 vacuum. One also can find that the impedance provides more direct and convenient information about the instability than the wake function. Analysis with multiple gas species provides the way to study the effect of realistic vacuum and understand the contribution from each of them. The effect of different gas species, such as CO and CO_2, can partially add together and contributes a broad spectrum and multiple spikes in the spectrum, which agrees with the measurement. The single gas model can't explain the multiple spikes in the measured spectrum. Therefore, it is important to analyse and simulate the beam ion instability with realistic multiple gas species. In some case, for instance in the ILC damping ring [11], the H_2 ion can even provide damping to the most unstable modes.

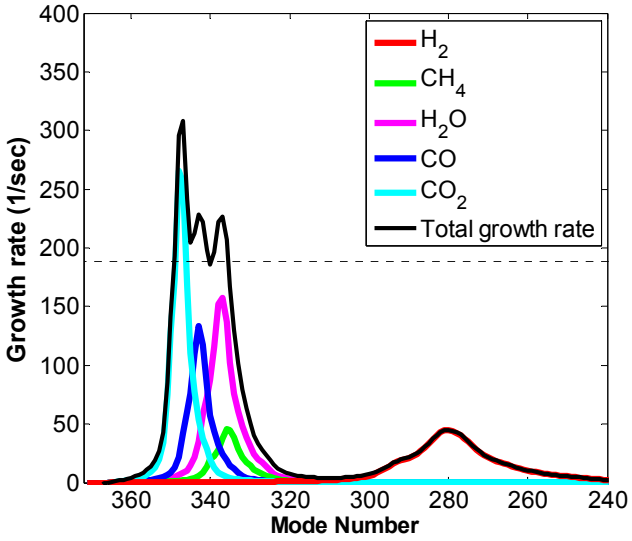

FIG. 10. The growth rate of unstable modes driven by various types of ion species. The beam current is 500mA with six bunch train beam filling pattern. The total vacuum pressure is 0.37*nTorr* . The dashed line in the growth rate plot shows the radiation damping rate. The chromaticity is zero in this case.

3.3. Bunch train effect

The mechanism of suppression of beam ion instability with multiple bunch train filling pattern is discussed in great detail in reference [10]. Roughly speaking, a multiple bunch train beam filling pattern can reduce the ion density near the beam and therefore the ion impedance, which is proportional to the ion density. The ion density during the bunch train gap decays exponentially with a decay time on the order of the ion oscillation period. If the bunch train gap is much longer than the ion oscillation period, we can assume all ions are cleared up after such a gap. The optimized bunch train gap is one or two ion oscillation periods in order to minimize the density of trapped ions and accommodate as many bunches as possible.

Fig. 11 shows the calculated impedance of the ion cloud and the growth rate of beam instability driven by ions with different beam filling patterns. It clearly shows the reduction of the impedance from using multiple bunch train filling patterns. The four and six bunch train have similar impedance, which agrees with the measurement and the simulation shown later. There is a weak instability with four and six bunch trains if including radiation damping as shown by the dashed line in the plot. The unstable modes near mode number 280 are driven by H_2 ions. These modes are completely damped by radiation damping when a multiple bunch train is used. However, H_2 can cause very weak instability for a single bunch train with 500 mA beam current. We rarely observe the unstable modes

driven by H_2 ion in SPEAR3. The frequency range of the unstable modes also agrees with the measurements. The analysis agrees with the measurements in many ways.

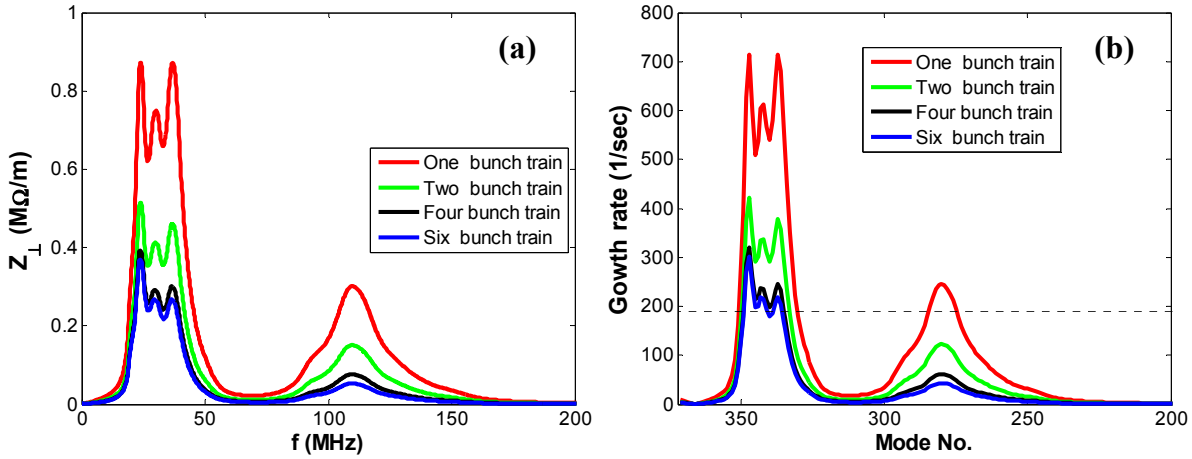

FIG. 11. Impedance of ion cloud (a) and growth rate of beam ion instability (b) with different beam filling patterns. The beam current is 500mA and the total vacuum pressure is 0.37*nTorr* in all cases. The chromaticity is 2.0. The dashed line in the growth rate plot shows the radiation damping rate.

3.4. Effects of bunched beam and chromaticity

The above analyses are done with a single particle model. For a bunched beam, the interaction force depends on the product of the impedance and the bunching factor. The effective impedance of a bunched beam is given by

$$Z_\perp^{eff} = \sum_{p=-\infty}^{\infty} Z_\perp(\omega) e^{-(\omega-\omega_\xi)^2\sigma_z^2/c^2} . \tag{7}$$

Here the chromaticity frequency $\omega_\xi = \omega_0\xi/\eta$ is the frequency shift due to the chromaticity $\xi = \Delta Q/(\Delta p/p)$, σ_z is the *rms* (root mean square) bunch length, η is the slippage factor defined as $\eta = \alpha - 1/\gamma^2$ and α is the momentum compaction factor. With zero chromaticity, the effective impedance of a bunched beam is almost the same as that of a single particle beam because of the low frequency of the ion cloud impedance. Therefore the above analyses are also accurate for a bunched beam. However, a non-zero chromaticity induces frequency shift and reduces the effective impedance seen by the beam. The reduction effect depends on both the bunch length and the chromaticity frequency. It is more effective for machines with a low momentum compaction factor and a long bunch length.

In the nominal operation of SPEAR3, both horizontal and vertical chromaticity is 2.0. When beam ion instability appears, which often happens at the beginning of a run after a long shut down, a slightly higher vertical chromaticity

is used to completely suppress the instability. The analysed mitigation effect of the beam instability with a larger chromaticity is clearly shown in Figure 12. The beam has a single bunch train filling pattern. The weak instability driven by hydrogen ions can be completely damped by a large chromaticity with the help of radiation damping. The growth rate of unstable modes driven by other ion species are supressed by a factor of more than 2. Note that one should look at the growth rate above the radiation damping rate (the dashed line in the plot) in order to compare with the measurements shown in Fig. 8. The frequency range of the calculated impedance shown in Fig. 11a also agrees with the measurement.

The vertical chromaticity effect for six bunch train beam filling pattern with 500mA beam is shown in Fig. 13. The weak instability driven by hydrogen ion is completely suppressed by radiation damping. A chromaticity of 4.0 suppresses all unstable modes except the modes driven by CO_2 ion. A chromaticity of 2.6 damped the most unstable mode in one of our measurements. The comparison with the analysis indicates that either the real total pressure is below 0.375 *nTorr* or the CO_2 gas in the vacuum is less that 14% since the most unstable mode in Fig. 13 is driven by CO_2. Our analysis is very close to the measurements even with the uncertainty of the vacuum. In the runs of last year with 300 *mA* and vertical chromaticity of 2.0, there is no instability. This also agrees with analysis.

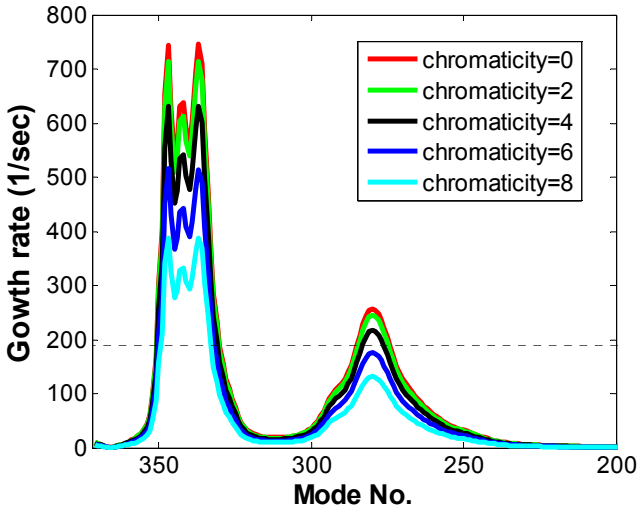

FIG. 12. Calculated growth rate of the beam ion instability in SPEAR3 at different chromaticity. A total vacuum pressure of 0.375 *nTorr* is used. The beam has a single bunch train, which consists of 280 bunches with a total beam current of 500 *mA*. The dashed line shows the radiation damping rate.

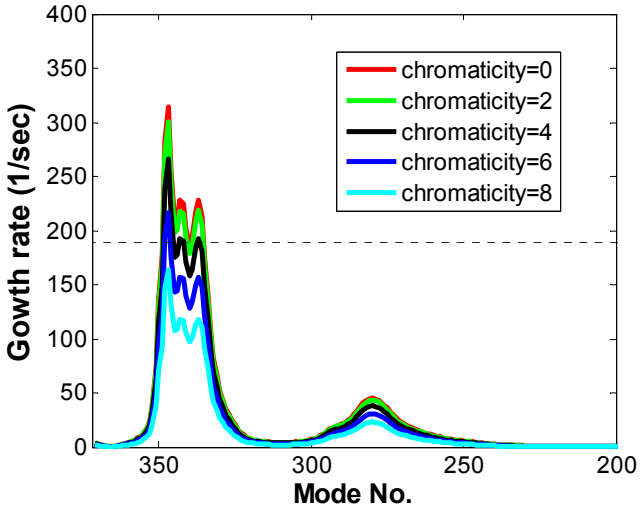

FIG. 13. Growth rate due to ions for six bunch-trains beam filling pattern. The most unstable mode is driven by CO_2 ion. The peak near mode 280 is driven hydrogen ions. The beam current is 500mA.

3.5. Emittance effect

One may notice that the distribution of unstable modes is similar to the distribution of impedance as shown before. Indeed, they are closely related. Now we look at it in detail. For a resonance-type wake function shown in Eq.(1), the Fourier Transform gives the impedance in the frequency domain as

$$Z_{ion}(\omega)=\frac{\hat{W}_t}{\omega}\kappa\frac{Q}{1+iQ\left(\frac{\omega_i}{\omega}\frac{1}{\kappa}-\frac{\omega}{\omega_i}\kappa\right)}\approx\frac{\hat{W}_t}{\omega}\frac{Q}{1+iQ\left(\frac{\omega_i}{\omega}-\frac{\omega}{\omega_i}\right)} \quad . \tag{8}$$

Here $\hat{W}_t$ and Q are the amplitude and quality factor obtained by fitting the wake function given by Eq. (4) according to the resonance model in Eq. (1). The factor $\kappa=\sqrt{1-(1/2Q)^2}\approx 1$ with Q≥4. At the resonance, $\omega=\omega_i$, the real part of the effective impedance can be simplified to

$$\mathrm{Re}\left\{\sum_{p=-\infty}^{\infty}Z_{ion}((pM+\nu_y+\mu)\omega_0)\right\}=\mathrm{Re}(Z_{ion}(\omega_i))\approx\frac{\hat{W}_t}{\omega_i}Q=\frac{4}{3}Q\frac{N_iS_b}{N_e}\frac{1}{\sigma_y(\sigma_y+\sigma_x)} \quad . \tag{9}$$

In our case, the beam is flat one with $\sigma_x >> \sigma_y$, therefore the peak impedance is inversely proportional to the product of horizontal and vertical beam size. The emittance affects the ion impedance in several ways for a given bunch current and bunch spacing. First, the peak impedance is roughly proportional to $1/\sigma_y$ if the coupling is smaller than a few percent and the number of ions is fixed. However, the number of trapped ions depends on the

beam emittance and the ion species. More ions can be trapped with a larger emittance. The heavier ions are more stable and have more chance to survive from the bunch train gap. These two factors make the heavier ions more important for a larger emittance. The reduction of the impedance with a larger emittance is smaller for heavier ions as shown in Fig. 14 for different coupling cases. The ratio of the coupling in these two cases is 10. The impedance of hydrogen ions is reduced by a factor about square root of 10. One the other hand, the reduction is small for heavier ions, for instance, CO_2 ions. There is a smaller frequency spread with a larger emittance as shown in the figure. This is another important feature of the emittance effect. The impedance frequencies decrease with a larger emittance. However, the relative frequency spread doesn't change with emittance. Therefore frequency spread $\Delta\omega = \omega_i / Q$ becomes smaller for a larger emittance. The weak instability and small frequency spread with a larger emittance shown in Fig. 4 agrees well with the theory.

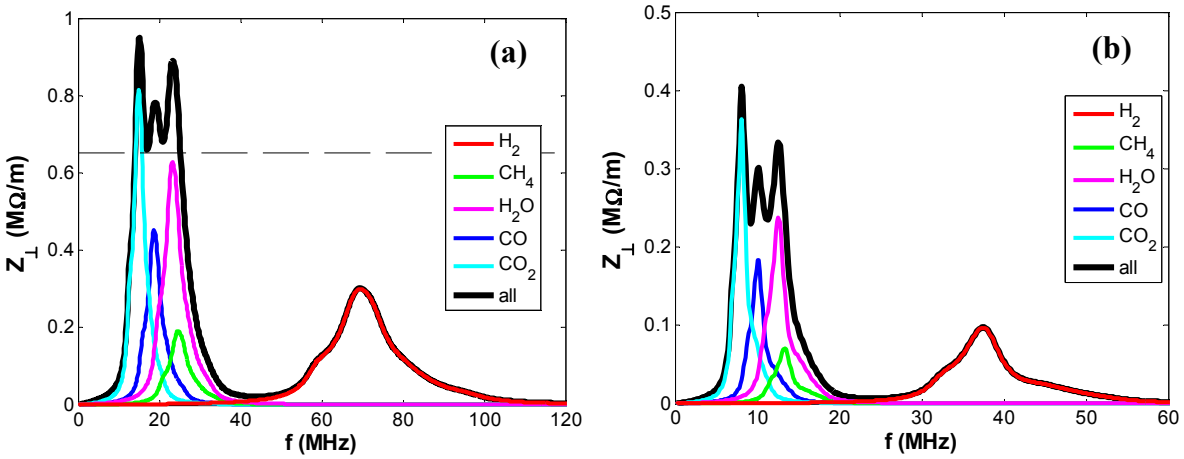

FIG. 14. Impedance of ion cloud with a coupling of 0.14% (a) and 1.4% (b). The beam has single bunch train with a total beam current of 200mA. The total vacuum pressure is 0.37*nTorr* in all cases. The dashed line shows the instability threshold due to the radiation damping. There is no instability with a coupling of 1.4%.

3.6. Beam Current effect

For a given beam filling pattern, the growth rate is proportional to the beam current and the ion impedance as shown in Eq. (6). It is easy to think that the ion impedance linearly increases with beam current. Actually, the ion impedance doesn't increase with beam current, and even slightly reduces with it. The number of ions increases with beam current. On the other hand, the frequency of the ion also increases. The peak impedance is inversely proportional to the frequency. This factor reduces the impedance with high beam current. The final ion impedance is

roughly proportional to N_i/N_e as shown in Eq. (9). For a single bunch train with long gaps, this ratio is a constant, which is proportional to the vacuum pressure. In this case, the ion impedance doesn't change with beam current, as long as the ions can be trapped along the bunch train ($\omega_i S_b/c<<1$). For a multiple bunch train case, the ratio of N_i/N_e becomes smaller with a high beam current because the ions have less chance to survive from the bunch train gap with a stronger beam force [10]. Fig. 15 shows the impedance dependence on the beam current for one and six bunch train beam filling pattern. The amplitude of the impedance has weak dependence on the beam current for a single bunch train beam. However, with a six bunch train beam, the impedance amplitude, especially at low frequency, decreases with beam current. In this case, the bunch train gap is not long enough to clear the ions.

As a result, the increase of the instability growth rate with beam current is linear or slower than linear for a given vacuum pressure. However, the pressure in general increases with beam current in a real beam vacuum chamber. Similar to the emittance effect, there is a larger frequency spread for a high beam current. The growth rate in Fig. 5 case is expected to be proportional to the beam current.

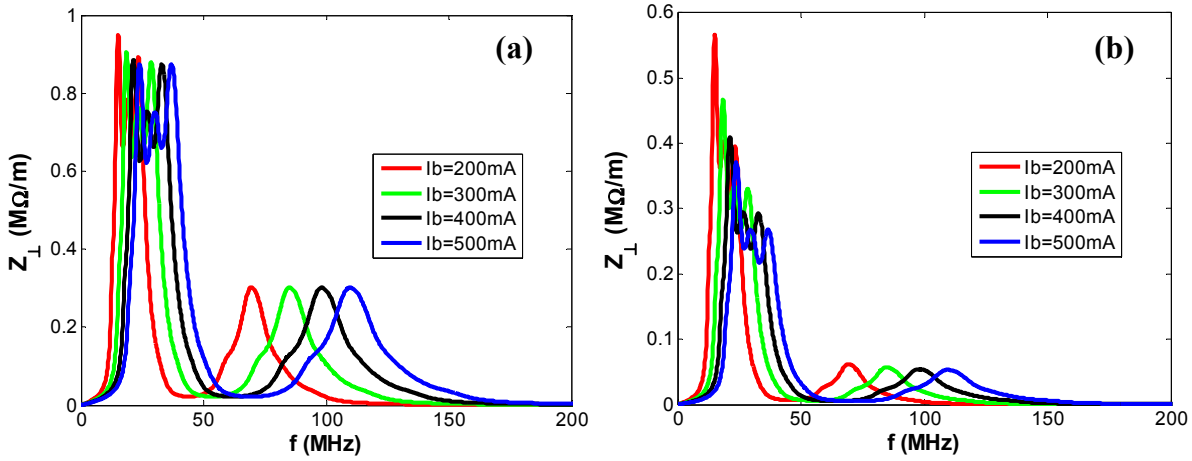

FIG. 15. Dependence of impedance on beam current for single bunch train beam (a) and six bunch train beam (b).

3.7. Effects of nonlinear space charge force and beam optics

Both the nonlinear space charge force and the beam size variation due to the beam optics provide damping to the beam ion instability. Therefore, it is interesting to investigate their damping effects independently. The comparison of the effects of nonlinear space charge force and beam optics is shown in Fig. 16. Three cases are compared: (1) with nonlinear space charge force only; (2) with beam optics effect only; (3) with both effects. The nonlinear space charge force is turned on and off by a low Q_0 of 9 and a high Q_0 of 200, respectively. The beam optics effect is

included or excluded by using a varying or constant beam size, respectively. In the case of a constant beam size, an average betatron function is used to calculate the beam size. The figure shows that the nonlinear space charge force and the beam optics effect have a similar damping effect on the beam ion instability in SPEAR3.

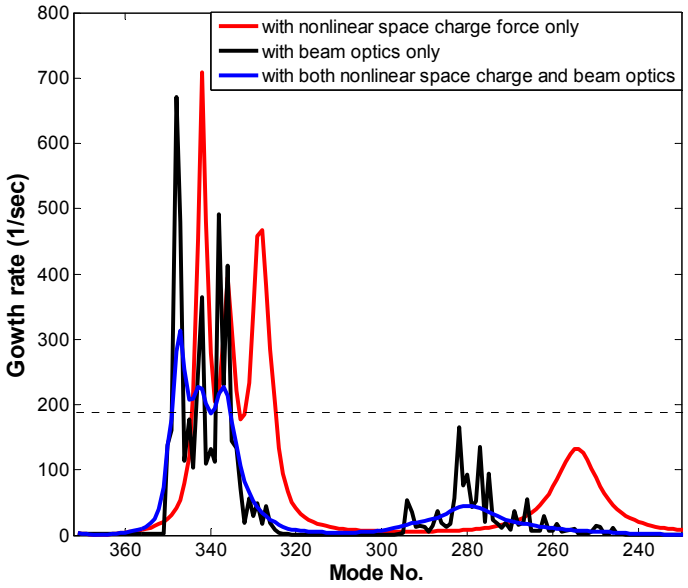

FIG. 16. The growth rate of beam instability in SPEAR3 with different effects: with nonlinear space charge effect only; with beam optics effect only and with both nonlinear space charge force and beam optics effects.

It is important to quantify the ion oscillation frequency spread due to the beam optics. It is represented by a Q factor in [10] and frequency spread [8]. However, it is not clear how to accurately calculate them for a given beam optics because the distribution of the ion frequencies usually is far from the standard distribution, such as Gaussian distribution. For instance, the calculated *rms* relative frequency spread in SPEAR is 100%, which is too large compared with the instability study in previous section. The traditional quality factor Q is defined as

$$Q = \frac{\omega_0}{\Delta\omega_0}. \tag{10}$$

Where $\Delta\omega_0$ is the full width at half maximum (FWHM). One may approximately estimate the Q factor due to beam optics as the ratio of average frequency along the ring $\overline{\omega}$ to the stand derivation σ_ω

$$Q_{optics} \approx \frac{\overline{\omega}}{\sigma_\omega}. \tag{11}$$

For instance, the estimated Q factor of the CO ion shown Fig. 9 is 9.86. This is a simple way to estimation the Q factor. Here we provide one alternate method to accurately estimate the Q factor and frequency spread due to the beam optics. For a ring with small variation in beam size, like SPEAR3, the wake function due to single ion species along the whole ring still has the resonance form as shown in Fig.9a. In this case, the wake function due to the ions along the whole ring can be written in the following form

$$W_{ring}(s) = W_0 e^{-\frac{\omega_r s}{2Q_{ring}c}} \sin(\frac{\omega_r s}{c}) = \left[W_0 e^{-\frac{\omega_r s}{2Q_0 c}} \right] e^{-\frac{\omega_r s}{2Q_{optics}c}} \sin(\frac{\omega_r s}{c}) . \quad (12)$$

where Q_{ring} is the Q factor of the wake function due to the ion cloud along the whole ring and Q_{optics} is due to the variation of beam size along the ring. We can get the following relationship from the above equation

$$\frac{1}{Q_{ring}} = \frac{1}{Q_0} + \frac{1}{Q_{optics}} . \quad (13)$$

The Q factor Q_{ring} can be found by fitting of the wake function along the whole ring. For the wake function of each type of ion species shown in Fig.9a, we get Q_{ring} =4.49 by fitting and Q_{optics} =8.9 from the above equation. Note that the Q_{optics} in SPEAR3 is close to Q_0 of 9.0 due to the nonlinear space charge effect. This finding agrees with the analysis where the beam optics and nonlinear space charge force contribute a similar damping to the instability. The Q_{optics} represents the relative variation of the ion frequency due to the beam optics effect. It doesn't vary with ion species, as expected.

IV. SIMULATIONS

Simulations have a number of advantages in the study of beam-ion instability: the nonlinearity of the ion-cloud force is automatically included; the effects of beam optics and bunch-train gap with arbitrary beam filling pattern can be easily handled; a realistic vacuum model with multi-gas species is straightforward in simulation. A Particle in Cell (PIC) code based on a wake-strong model is used here [10].

Fig. 17 shows the simulated beam instability with different beam filling patterns with total beam current of 500 *mA*. The total vacuum pressure is 0.37 *nTorr* for all the simulation in this section. There is a fast instability in the linear regime and it is slowed down by the nonlinearity of space charge force when the amplitude is larger than the beam size. The instabilities with four and six bunch train are very similar. The simulations agree with the measurement. The six bunch train filling pattern is the optimum one, which gives a growth time of 2.72 *ms* with a

pressure of 0.37 *nTorr*. This agrees well with the analytical model in which the calculated fastest growth time is 3.18 *ms*. The growth time in the experiment is unknown. However, it is known that there is a weak instability with six bunch train beam filling pattern, which suggests a growth time slightly shorter than the radiation damping time of 5.3*ms*. The simulation is within a factor of two of the measurements.

Fig.18 shows the evolution of vertical oscillation amplitude of electron bunches with a six bunch-train filling pattern. The overall amplitude grows exponentially with time except at the beginning when the instability starts. The instability is still in an exponential regime after 20 *ms* due to its slow growth.

With simulation, it's easier to study the nonlinear regime. This is one of the advantages of simulation over the analysis. Fig. 19(a) shows the unstable mode with a single bunch train beam. Instead of mode number, the frequencies of modes are given in order to compare with the frequencies of the impedance. The unstable modes have frequency below 50*MHz*. Three peaks are clearly seen, which agrees with the impedance and unstable modes shown in Fig.11. However, the unstable modes driven by Hydrogen ion are hard to see. There are weak signals shown in the Hydrogen's frequencies. This agrees with measurements, where we rarely see sidebands driven by Hydrogen ions. A particular mode 336 is shown in Fig 19(b). The vertical axis has a logarithmic scale. Both the linear and nonlinear regime are clearly seen. The mode has exponential growth when its amplitude is less than 10 *um*, thereafter it grows linearly. The mechanism of saturation at the order of the beam size explains the small amplitude in the measurements.

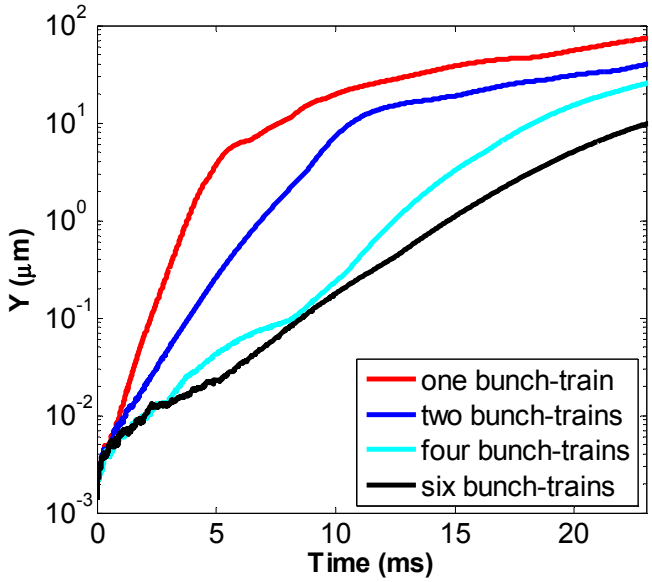

FIG. 17. Simulated beam ion instability for different beam filling patterns. The total beam current is 500 *mA* with total bunch number of 280 in all cases. Zero chromaticity and total vacuum pressure of 0.37 *nTorr* are used in the simulation. The radiation damping is not included.

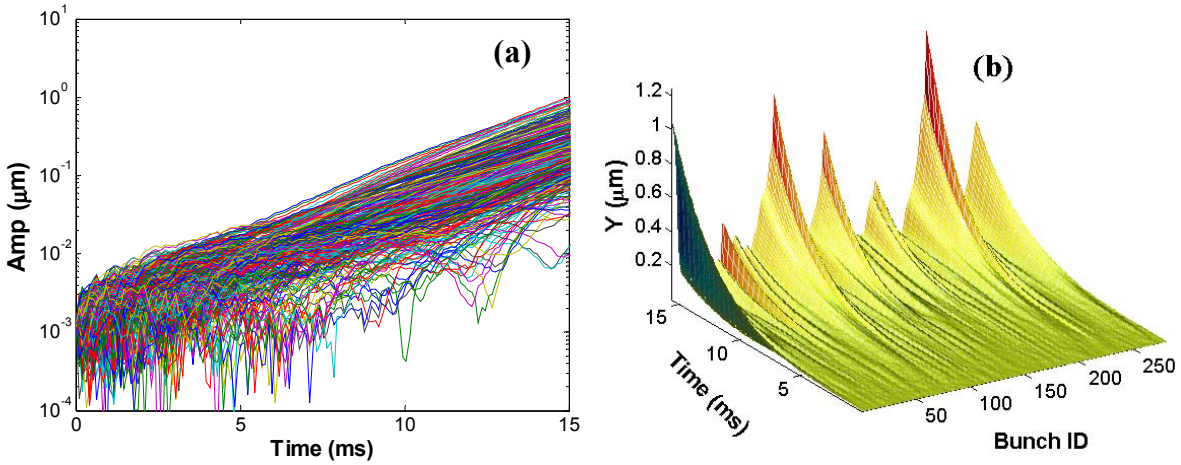

FIG. 18. Simulated vertical beam ion instability for six bunch-train beam filling pattern: 2D plot (a) and 3D plot (b) of the growth of vertical amplitude. The vertical oscillation amplitude in (a) is in logarithmic scale, while it is in linear scale in (b). The different lines in (a) are for different bunches. The total beam current is 500mA with total bunch number of 280.

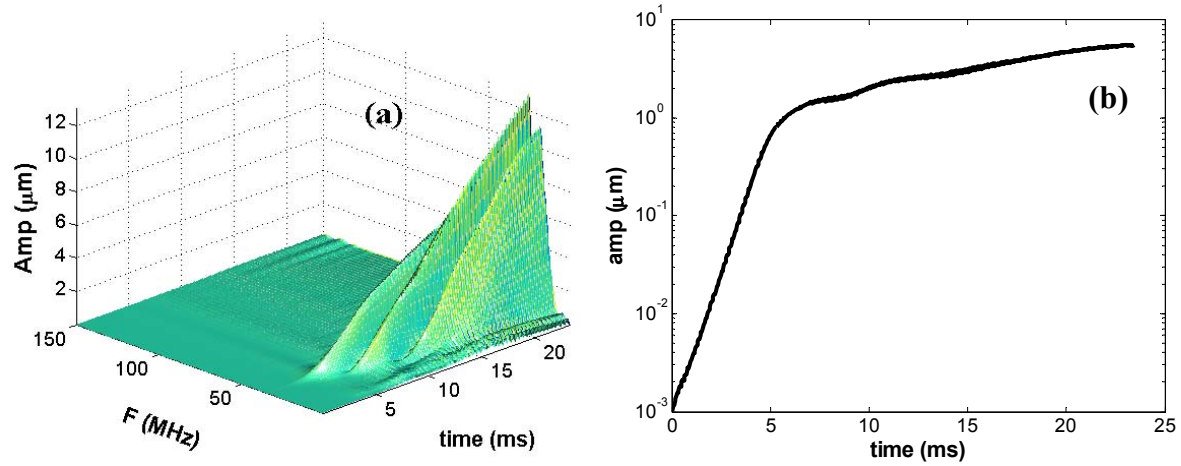

FIG. 19. All unstable modes (a) and a particular unstable mode 336 (b) for single bunch train filling pattern with the same parameters in Fig.17. Instead of unstable mode number, the frequencies of the unstable modes are shown in (a) for direct comparison with the frequency of impedance. Radiation damping is not included.

CONCLUSIONS

This paper summarizes the comprehensive measurements, analyses and simulations of the beam-ion instabilities in SPEAR3. A vertical instability has been first observed with nominal vacuum pressure when a single bunch train beam is filled. It varies with vacuum pressure and beam emittance, which directly confirms that the instability is driven by ions in the vacuum chamber. The instability causes the beam to oscillate with an amplitude order of the *rms* beam size. A blow-up of the beam emittance has been observed when the bunch-train gap is very short. Besides vacuum pressure, the instability is sensitive to the beam emittance, filling pattern and chromaticity. Multi-bunch train filling pattern is very helpful to suppress the instability. Six bunch-train is the optimized beam filling pattern and the optimized bunch train gap is about 1~2 ion oscillation wavelengths. Now SPEAR3 operates at 300mA without instability by applying a beam filling pattern of six bunch-trains. The instability appears at 500mA even with six bunch-trains filling pattern, which can be completely suppressed by a slightly larger chromaticity. However, a large chromaticity reduces the beam lifetime and injection rate.

We analyse the multi-bunch train beam ion instabilities with the SPEAR3 beam optics, multi-gas species vacuum, nonlinear space charge force and realistic beam filling pattern together. All these factors provide damping to the instability. The damping of the beam ion instability due to beam optics can be clearly seen in the analysis. The nonlinear space charge force also plays an important role in the damping of the beam ion instability; in SPEAR3 it has a similar damping effect as the beam optics. The multiple spikes in the beam spectrum can be well explained by our multiple gas species vacuum model.

We introduce the impedance model in the study of beam ion instability for the first time. The impedance of the ion cloud is broadband due to the variation of beam size along the accelerators and the multiple gas species in the vacuum. The impedance provides clear information for understanding the ion instability, the effect of beam optics and multiple gas species in the vacuum.

There are excellent agreements between our analyses and simulations. All the measurements can be well explained by analyses. Our analyses and simulations agree with the measurements in many ways. For instance, the frequency of the measured beam spectrum agrees well with our analyses and simulations. The calculated growth rate of beam ion instability with multi-bunch train is very close to the simulation. The agreement between simulation and experiment is within a factor of 2.0, even with the uncertainty of the real growth rate in the measurements. The

observed mitigation of the beam ion instability with multiple bunch trains can be well explained by our analysis and simulation.

ACKNOWLEDGEMENTS

We would like to acknowledge the SPEAR3 operation team for its help on the measurements and thank Rodney Pak for providing the vacuum data. We also thank D. Teytelman for providing the bunch-by-bunch data.

REFERENCES

[1] T. O. Raubenheimer and F. Zimmermann, Phys. Rev. E **52**, 5487 (1995).

[2] J. Byrd, et al., Phys. Rev. Lett. 79, 79(1997).

[3] J. Y. Huang, et al., Phys. Rev. Lett. 81, 4388 (1998).

[4] M. Kwon, et al., Phys. Rev. E 57, 6016 (1998).

[5] H. S. Kang, et. al., in *Proceeding of 2006 European Particle Accelerator Conference, Edinburgh, UK,* 2771(2006)

[6] R. Nagaoka, et al., in *Proceedings of 2007 Particle Accelerator Conference, Albuquerque, USA,* 2019(2007)

[7] B. Jiang, et. al., Nucl. Instrum. Meth. A 614, 331(2010)

[8] G. V. Stupakov, KEK Proceedings 96-6, 243 (1996)

[9] E.S. Kim and K.Ohmi, Japanese Journal of Applied Physics 48, 086501 (2009)

[10] L. Wang, Y. Cai, T. O. Raubenheimer and H. Fukuma, Phys. Rev. ST Accel. Beams 14, 084401 (2011)

[11] L. Wang, M. Pivi, T. O. Raubenheimer and J. Safranek, SLAC-PUB-15353(2013)

[12] A. Chao, "Physics of Collective Beam Instabilities in High Energy Accelerators", Wiley, (1995).